Acoustic Nonlinearities and Power Losses at Orifices

A. Cummings*
University of Missouri-Rolla, Rolla, Missouri

Acoustic power losses occur when high-amplitude sound waves impinge on an orifice in the absence of mean flow. Described is a simple theoretical model of these losses, in which a harmonic, linear acoustic field is coupled to a nonlinear hydrodynamic flowfield at the orifice. Experimental and theoretical data on power losses at orifices with both ρc and flanged acoustic terminations are compared, and fairly good agreement is noted. The structure of the flowfield in the neighborhood of the orifice is broadly described and some quantitative comparisons are made between the measured translational velocity of the ring vortices shed from both sides of the orifice and theoretical predictions. Again, the theory is seen to give generally reasonable results.

Nomenclature

A = cross-sectional area of pipe
A_0 = orifice area
a = orifice radius
C_c = contraction coefficient
c_0 = speed of sound
f = frequency
I = impulse of vortex
k_0 = ω/c_0, wave number
L = length of a slug of fluid
L_p^i = sound pressure level in incident wave
P_i = sound pressure amplitude in incident wave
R = distance of observer from orifice
$\hat{R}e$ = Reynolds number based on $\hat{v}$ and a
R_v = radius of vortex
r = radial coordinate
$\hat{S}$ = Strouhal number based on $\hat{v}$, a and ω
T = kinetic energy of vortex
t = time
V_v = translational velocity of vortex
V_1 = amplitude of fundamental component of orifice velocity
v = fluid velocity in orifice
$\hat{v}$ = peak fluid velocity in orifice
v_{eff} = effective velocity
v_x = axial component of velocity
W_{abs} = sound power absorbed at orifice
W_i = sound power in incident wave
W_r = sound power in reflected wave
W_1 = net sound power on source side of orifice
W_2 = transmitted sound power
x = distance of vortex from orifice plate
α = nondimensional vortex radius
Γ = total circulation of vortex
Δ_L = net acoustic power loss
Δ_T = acoustic transmission loss
Δ_R = acoustic reflection loss
δ = mass end correction of orifice
ζ_1 = nondimensional orifice impedance
θ_{NL} = nondimensional nonlinear orifice resistance
θ_r = nondimensional radiation resistance
ν = kinematic viscosity of fluid
ρ_0 = fluid density
σ = A_0/A, porosity of orifice plate
ω = $2\pi f$, radian frequency

Presented as Paper 83-0739 at the AIAA 8th Aeroacoustics Conference, Atlanta, Ga., April 11-13, 1983; submitted May 5, 1983; revision received Aug. 8, 1983.

*Associate Professor, Mechanical Engineering Department. Member AIAA.

I. Introduction

In recent years, there has been considerable interest in the acoustic power losses that occur as a result of the interaction between acoustic fields and shear layers in separated flows. Of special importance has been the energy dissipation observed to take place at low frequencies when sound waves are transmitted out through a nozzle from which a gas jet is issuing. Bechert et al.[1] and Ahuja and co-workers[2] have reported experimental investigations of this effect and Bechert,[3] Howe,[4,5] and Reinstra[6] have given theoretical analyses that are in generally good agreement with the measured data. The mechanism of the energy absorption is the conversion, via acoustic interaction with a shear layer, of acoustic energy into vortical energy and its subsequent dissipation into heat without significant acoustic regeneration.

It is also possible for this power loss mechanism to occur in the absence of mean flow if the acoustic velocity amplitude is high enough, since the acoustic boundary layer can then separate at a sharp edge and the velocity field will interact with the shear layer thus formed, producing vortices that absorb energy from the sound field and undergo viscous dissipation processes. Salikuddin and Plumblee[7] reported measurements of power losses at various types of duct terminations, while Cummings and Eversman[8] offered a theoretical model by way of explanation, the results of which are in quite good agreement with Salikuddin and Plumblee's data. Cummings[9] has carried out an independent experimental investigation of acoustic absorption at orifices, using tone-burst signals (Salikuddin and Plumblee, by contrast, used "broadband" transient signals, Fourier transformed to give data in the frequency domain), and has also related the acoustic losses to the characteristics of the ring vortices produced at either side of the orifice.

The nonlinear acoustic behavior of orifices at high amplitudes has, of course, been known for many years, but it is only recently that the associated energy dissipation has been studied.

The purpose of this paper is to report an extension of the work described in Ref. 9. Acoustic power losses associated with an orifice plate placed at the end of a uniform pipe have been measured. Both ρc and flanged terminations have been used so that the effects of the essentially different impedance conditions could be demonstrated. Experimental data on the

orifice flowfield have also been obtained. Comparisons between theoretical and experimental data have been made where appropriate.

II. Theory

The two topics of interest here, sound power losses at orifices and vortex formation, will be discussed separately.

Acoustic Dissipation at an Orifice

The theoretical arguments pertaining to the acoustic losses at the orifice have been discussed in Ref. 9 and are essentially similar to those described in detail by Cummings and Eversman[10]; accordingly, only the salient points will be touched on here. The physical arguments are as simple as possible, with the number of arbitrary assumptions kept to a minimum. It might have been more satisfying to have utilized the excellent and very detailed analysis of Hersh and Rogers[11] describing the orifice impedance at both low and high amplitudes, but this requires the use of an empirically determined discharge coefficient that would be considered a drawback in the context of the present treatment.

Figure 1 shows a circular pipe terminated in an orifice plate, which may be part of an infinite flange (as shown) or alternatively might have a further length of pipe attached at its right-hand side, so as to constitute a termination with ρc impedance.

Since there is no mean flow through the orifice, there will be an alternating acoustic flow, which produces ring vortices as shown in Fig. 2. These are generated on *both* sides of the orifice (this may be convincingly demonstrated by experiment).

A *vena contracta* is assumed to be formed on the outflow side of the orifice (following separation of the boundary layer at the lip) and here the flow streamlines can be assumed parallel. A short distance from the orifice, to its inflow side, the streamlines are again parallel, if the plane acoustic mode alone is assumed to propagate in the tube.

The flow is taken to be inviscid (aside, of course, from the viscous processes causing boundary-layer separation), and it has been shown[10] that the time-dependent Bernoulli equation may be used to relate the acoustic field to the flow velocity in the orifice. An essential feature of this approach is that "pressure recovery" (caused by deceleration of the fluid at the outflow side of the orifice) does not occur. Apart from this assumption, no details of the flowfield are required. Although the sound wave incident upon the orifice may be taken to be harmonic, it is clear that (at high amplitudes) neither the reflected wave nor the transmitted wave will be so. Both theory and experiment, however, indicate that the distortion will generally be small enough for a linear analysis still to be of use. The particle velocity in the orifice will also suffer from harmonic distortion, since it is (roughly speaking) proportional to the square root of the pressure differential

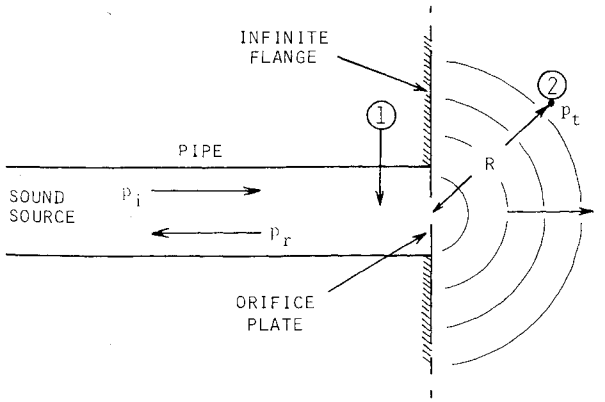

Fig. 1 Sound transmission through an orifice from a pipe.

across the orifice. Even so, the velocity in the orifice may be taken to be represented, approximately, by its fundamental component, so that a harmonic representation of the overall behavior of the system may be retained. The nondimensional acoustic impedance of the orifice, at point 1 in the tube, can be shown[10] to

$$\zeta_1 = (\theta_{NL} + ik_0\delta + \theta_r)/\sigma \tag{1}$$

(if the relatively small viscous losses at the orifice are neglected), where θ_{NL} is a nonlinear resistance, given by

$$\theta_{NL} = V_1(1-\sigma^2 C_c^2)/2.464C_c^2 c_0 \tag{2}$$

where δ is the total (inner + outer) "mass end correction" and θ_r the radiation resistance on the outer side of the orifice. The contraction coefficient C_c (equal to the area of the *vena contracta* divided by the orifice area) is taken to have the typical steady flow value of 0.61. The fundamental component of the orifice velocity V_1 is obtained by numerical solution of the equation

$$\sigma\rho_0 c_0 V_1 |1+\zeta_1| - 2|P_i| = 0 \tag{3}$$

where P_i is the pressure amplitude in the incident wave. The incident and reflected acoustic powers on the source side of the orifice are given by

$$W_i = A|P_i|^2/2\rho_0 c_0 \tag{4a}$$

$$W_r = -|\zeta_1 - 1|^2 W_i/|\zeta_1 + 1|^2 \tag{4b}$$

the net power being $W_1 = W_i + W_r$; the transmitted power is given by

$$W_2 \simeq \rho_0 c_0 \theta_r A_0 V_1^2/2 \tag{5}$$

Three quantities of interest concerning power flow are as follows:

$$\text{Net acoustic power loss } \Delta_L = 10\log(W_1/W_2) \tag{6a}$$

$$\text{Orifice transmission loss } \Delta_T = 10\log(W_i/W_2) \tag{6b}$$

$$\text{Orifice reflection loss } \Delta_R = 10\log(W_i/W_r) \tag{6c}$$

Appropriate expressions for θ_r and δ in Eq. (1), for the two types of termination considered here, are:

$$\rho c \text{ termination: } \theta_r = \sigma,\ \delta = 0.85a \tag{7a}$$

$$\text{Flanged termination: } \theta_r = (k_0 a)^2/2,\ \delta = 0.85a \tag{7b}$$

(The mass end correction on the outflow side of the orifice is assumed to be zero at sufficiently high amplitudes.)

By inserting Eq. (7) into Eq. (1) and performing the necessary manipulations, values of Δ_L, Δ_T and Δ_R may be calculated for any given geometry and value of P_i.

Generation of Vortices

About the only detailed discussions apparent in the literature concerning vortex production by sound waves at orifices (apart from the rather brief treatment in Ref. 9) are those reported by Ingard and Labate[12] and Disselhorst and Van Wijngaarden,[13] although the latter is concerned with unflanged duct terminations rather than orifices. Ingard and Labate gave a phenomenological classification of various flow regimes in terms of the nature of the local flow circulation near the orifice. They even achieved a tolerably good quantitative correlation between measurements of nonlinear

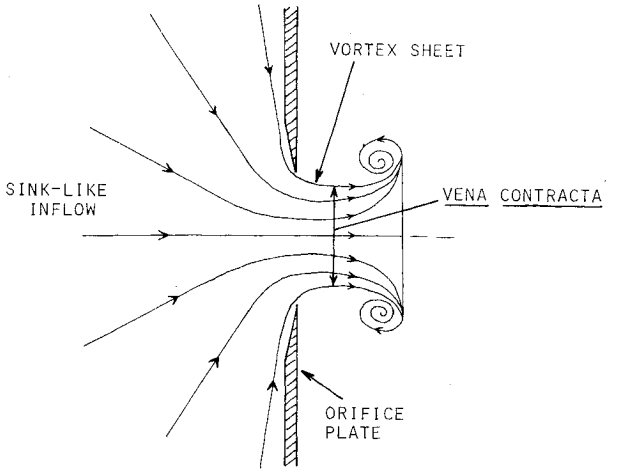

Fig. 2 Roll-up of a vortex at an orifice.

resistance based on impedance data and values inferred from measurements of the time-averaged force exerted by vortices on a small disk attached to a torsion balance. In terms of Ingard and Labate's flow regimes, the vortex systems discussed in this paper would be characteristic of their "region 4," in which ". . . .air is drawn in diffusely from one side of the orifice and thrown out along the axis on the other side. This effect alternates from one side to the other with the frequency of the sound, and the flow pattern is exactly symmetrical on both sides of the orifice."

Some sort of attempt is required to relate the acoustic field to the characteristics (total circulation Γ, kinetic energy T, translational velocity V_v, radius R_v) of the vortices produced by the acoustically induced orifice flow. Initially, calculations were made, based on the kinematics of the orifice flow, using a theoretical treatment of vortex roll-up discussed by Saffman.[14] The values of vortex kinetic energy thus obtained were at variance with both the measurements of the vortex velocities and (indirectly) the behavior of the orifice impedance; it is believed that wall effects are responsible for this disagreement, because Saffman's analysis is valid only for the rolling-up of a cylindrical vortex sheet in an *unbounded* fluid. This approach was abandoned, since the kinetic energy in the presence of a wall is difficult to calculate directly, and the following method was adopted.

The power absorbed in the fundamental component of the orifice velocity is given approximately by

$$W_{\text{abs}} \simeq A_0 \theta_{NL} \rho_0 c_0 V_1^2/2 \tag{8}$$

If $\sigma^2 C_c^2 \ll 1$, Eqs. (2) and (8) may be combined to yield

$$W_{\text{abs}} \simeq 0.203\, A_0 \rho_0 V_1^3/C_c^2 \tag{9}$$

If all of the absorbed power is converted into vortex kinetic energy, then $W_{\text{abs}} = 2fT$, since vortices are shed from both sides of the orifice. Equation (9) thus gives an expression for T in terms of V_1,

$$T \simeq 0.1015\, A_0 \rho_0 V_1^3/fC_c^2 \tag{10}$$

Standard inviscid vortex theory (e.g., see Saffman[14]) gives an expression for the translational velocity of a single vortex,

$$V_v = T/2\pi\rho_0 R_v^2 \Gamma + 3\Gamma/8\pi R_v \tag{11}$$

At this stage, several points are worth noting. The initial roll-up of a vortex takes place in the proximity of the surface of the orifice plate. In the absence of viscous losses, Kelvin's circulation theorem indicates that Γ should not vary and the first law of thermodynamics dictates that T should also be constant. When a vortex is still near the plate, however, there will be a velocity component directed toward its center, produced by a combination of the velocity field of the vortex itself and that of its image in the plate (see, for example, the discussion by Sommerfeld[15]). The nearer the vortex is to the plate, the larger will be the velocity component pointing toward its center and the smaller the translational velocity component. Thus, one would expect R_v to decrease and V_v to increase as the vortex moves away from the orifice and the influence of the image vortex diminishes. Observations confirm this reasoning. Under prevailing conditions of V_1 and f, vortices form near the orifice and V_v is relatively small. It can be seen that R_v falls away rapidly to a more or less constant value as the vortex proceeds away from the plate and the vortex spacing increases to a roughly constant value, showing that V_v had also increased. As an indication of the magnitude of "wall effects," one may calculate the axial velocity at the center of the real vortex (induced by the image vortex), as a fraction of the axial velocity at the center of the *isolated* real vortex in the absence of wall effects. Neglecting sign (since these two velocities are in opposite directions), one finds that this ratio is 0.01 when $x/R_v \simeq 5.1$ (x being the distance of the vortex from the plate), 0.05 when $x/R_v \simeq 1.6$, and 0.1 when $x/R_v \simeq 0.91$. A rough guide is that wall effects are small if $x/R_v > 2$, that is, the vortex is one diameter away from the wall; here, the induced velocity from the image is less than 4% of the vortex velocity. In the foregoing discussion, the interaction between successive vortices has been ignored. Of course, this can also be important. According to the above arguments, vortex/vortex interaction should be small if the vortex spacing is greater then about two ring diameters. Even at a spacing of one diameter, the interaction should be moderately small.

A consequence of the change in R_v and V_v, as the vortex moves away from the wall, is that the vortex impulse I is not conserved. If $x/a > 2$, however, I will be more or less constant and the vortex spacing (together with f) can be used as a measure of V_v. Equations (10) and (11) may be used to calculate V_v if R_v/a is known and the vortex spacing is not too small. Measurements of R_v in the present series of experiments were not considered sufficiently accurate to give useful information about the parametric dependence of R_v/a, but measurements of Maxworthy[16] and Liess and Didden[17] on the vortex radius were utilized as follows.

If the instantaneous velocity in the orifice is v and if v^2 is approximately proportional to the pressure drop across the orifice, one may show that the length of the slug of fluid ejected from the orifice during each flow half-cycle is given by

$$L = 0.759\pi\hat{v}/\omega \tag{12}$$

for a sinusoidal pressure variation, where the circumflex denotes a maximum value. Dimensional analysis leads one to expect that R_v/a is a function of $\hat{v}a/\nu$ and $\hat{v}/\omega a$, in other words, of Reynolds and Strouhal numbers. The limited experimental data of Maxworthy on the radius of single vortices produced by orifice plates may be combined with the more extensive combined data of Refs. 16 and 17 on the radius of vortices ejected from nozzles ($L/2R_v$ being a relevant parameter in both cases) to yield the empirical relationship

$$R_v/a \simeq 1.08 \hat{S}^{0.223} \hat{R}e^{0.035} \tag{13}$$

where $\hat{S}$ and $\hat{R}e$ are the Strouhal and Reynolds numbers (in slightly nonstandard form, as above) based on $\hat{v}$. Equation (12) has been used here to relate L to $\hat{v}$ and ω. Some uncertainty remains concerning the applicability of Eq. (13) to periodic vortex formation, but this will have to suffice in the absence of more relevant data.

In Eq. (11), Γ remains to be expressed in terms of easily measurable quantities. From the work of Didden,[18] one may

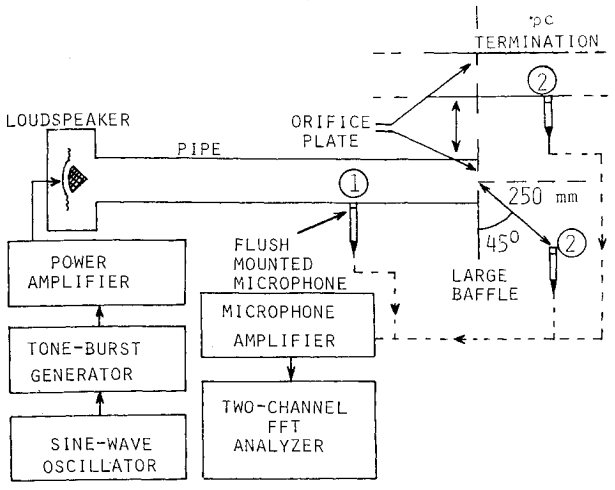

Fig. 3 Experimental arrangement for acoustic transmission tests.

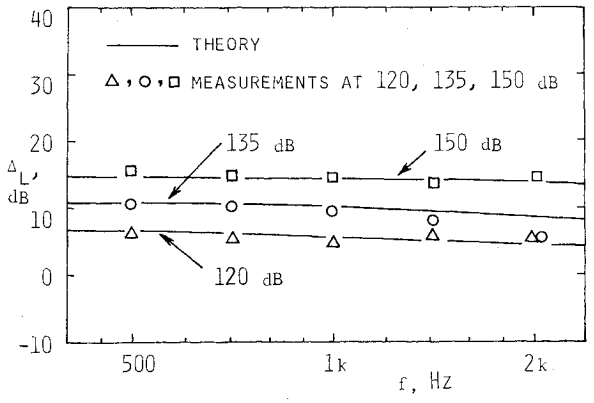

Fig. 4 Net power loss vs frequency for 3.3 mm orifice with ρc termination.

see that, for fluid ejected from a pipe containing one-dimensional flow, the vorticity flux from the internal boundary layer is given by

$$d\Gamma/dt = -\int_0^a (\partial v_x/\partial r) v_x dr \tag{14}$$

where v_x is the axial component of the velocity and r the radial coordinate. If a slug of fluid surrounded by a vortex layer or a thin shear layer is ejected from an orifice plate, and the effective fluid velocity of the slug is v_{eff}, the Eq. (14) may be utilized and integrated, first with respect to r and then with respect to t (over one-half period) to yield

$$\Gamma = \tfrac{1}{2}\int_0^{\pi/\omega} v_{\text{eff}}^2 dt \tag{15}$$

If v_{eff} is put equal to the fluid velocity in the *vena contracta,* then v_{eff}^2 is approximately equal to $\hat{v}^2 \sin\omega t/C_c{}^2$. Equation (15) then gives

$$\Gamma = \hat{v}^2/\omega C_c{}^2 \tag{16}$$

Equation (16) may be inserted into Eq. (11) and the result expressed in terms of $\hat{v}$,

$$V_v = 0.436\hat{v}/\alpha^2 + 0.119\hat{v}^2/\omega C_c^2 a \tag{17}$$

where $\alpha = R_v/a$; the relationship $V_l = 1.11\ \hat{v}$ has also been used (see Ref. 10). Equation (17) together with Eq. (13) enables V_v to be explicitly calculated as a function of $\hat{v}$ for given values of ω and a; this equation is valid provided the vortex spacing is greater than about one to two ring diameters.

III. Measurements

Figure 3 shows the arrangement for the acoustic transmission tests. An acoustical driver was fitted to one end of a 50.5 mm i.d. aluminum pipe. At the other end of the pipe, one of a series of sharp-edged orifice plates could be fitted. The acoustic termination to the right-hand side of the orifice plate was either a large baffle or a long pipe, also of 50.5 mm diam. The driver was fed with either two- or four-cycle tone bursts. A 13 mm condenser microphone placed at position 1 (on the source side of the orifice plate) or position 2 (on the transmission side of the plate) detected the sound pressure. The microphone was calibrated with a Bruel and Kjaer type 4220 Pistonphone. The microphone signal was fed via a microphone amplifier to a Scientific Atlanta SD375 analyzer, which permitted time-domain editing of the signal. The "desired" part of the signal was isolated by erasing the "unwanted" part. In the case of position 1, the desired portion of the signal was either the first incident or the first reflected pulse and, in the case of position 2, was the first transmitted pulse. The incident and reflected pulses were always distinct and no ambiguity was experienced in the signal editing. The Fourier transform of the edited signal was taken using the analyzer, with a "transient window" applied to the signal. The modulus of the pressure spectrum at the tone burst frequency was taken as being the essential characteristic of the signal.

The sound power in the signal was estimated from the modulus squared of the pressure spectrum multiplied by the area of the wave fronts at the measurement location. Of course, this included a constant of proportionality that disappeared in the acoustic power quotients defining Δ_L, Δ_T, and Δ_R in Eqs. (6).

Because of the nonlinear orifice impedance, the transmitted pressure signal was not exactly sinusoidal. Considerable harmonic distortion was evident at high incident pressure amplitudes in the case of the flanged termination, where the radiated pressure is proportional to $\dot{v}$; this exaggerates the effects of the higher harmonics. At lower amplitudes, particularly in the case of the ρc termination, the transmitted wave was almost sinusoidal. In some of the tests, the square of the peak-to-peak pressure was used in the sound power calculations rather than the pressure spectrum. This process was checked against the pressure spectrum method in selected cases and the two procedures gave almost identical results.

Incident sound pressure levels (based on the peak-to-peak pressure of the tone bursts) in the tests were 120-150 dB. Wave steepening effects were evident, particularly in the reflected waves at the higher amplitudes, but were not so severe as to influence the results significantly.

Measurements involving the vortices generated at the orifice plates were made using steady sinusoidal signals. A smoke generator, which produced a fine mist of hydrocarbon oil, was constructed and the smoke was injected near one side of the orifice plate so that it was drawn, in a laminar wall jet, into the orifice by the time-averaged streaming motion characteristic of high-amplitude orifice flow. Stroboscopic illumination made the vortices visible via the light scattered by the oil droplets and the vortex spacing was measured from video recordings of the flow pattern. The vortex convection velocity V_v was calculated as the product of the vortex spacing and the frequency. To reduce wall effects, the vortex spacing was measured from a point at least one vortex diameter from the orifice plate. Single-frame photographs of the vortices were also taken.

For convenience, the measurements on vortices were all made using the flanged duct termination. In some cases, the aluminum pipe from the driver was replaced by a Plexiglass tube of the same diameter, so that the vortex motion on the source side of the orifice could be observed.

The transmission side of the orifice was surrounded by a small anechoic enclosure to reduce the effect of acoustic reflections, and the radiated sound pressure was detected by means of a microphone. This microphone was placed so that it was in the direct acoustic field where the radiated sound pressure level fell by 6 dB per doubling of the distance from the orifice. The microphone signal was graphically recorded and the peak orifice velocity found as follows. The acoustic pressure radiated by the orifice is given by $\rho_0 A_0 \dot{v}/2\pi R$ (R being the distance of the observation point from the orifice) if the radiation is taken as being that of a monopole on a reflecting plane. It can easily be shown that the peak orifice velocity is given by $\pi R/\rho_0 A_0$ multiplied by the area between one pressure half-cycle and the time axis. This area was averaged over two half-cycles using a planimeter, thus giving an average value of $\hat{v}$ over one cycle.

IV. Experimental Data and Comparison with Theory

This section is subdivided into discussions concerning the acoustic transmission at orifices and the vortex formation.

Acoustic Transmission Characteristics

Figures 4-7 show experimental and theoretical data on Δ_L and Δ_T for two sizes of orifice with both ρc and flanged terminations; Δ_R is of somewhat less interest here and will not be considered.

In Figs. 4 and 5, Δ_L is shown for a 3.3 mm diam. orifice with (respectively) ρc and flanged terminations. Experimental data are given for incident sound pressure levels of 120, 135, and 150 dB. In Fig. 5, the measured Δ_L data at the lower levels and higher frequencies are not shown because the acoustic boundary-layer attenuation in the tube rendered the results unreliable and empirical corrections to the data proved unsatisfactory. Agreement between the measurements and theory is acceptably good. The most striking difference between the two sets of data is that Δ_L in the case of the ρc termination is hardly dependent upon frequency, while the flanged termination brings about an appreciable frequency dependence, Δ_L being largest at low frequencies. In both cases, the net power loss becomes greater as L_p^i increases; this is to be expected, since θ_{NL} will clearly be greater at high amplitudes.

In the case of the ρc termination, ζ_1 is only weakly frequency dependent except at high frequencies and low amplitudes, since neither θ_{NL} nor θ_r is frequency dependent. This explains why Δ_L is almost constant with frequency, especially at high amplitudes.

By contrast, θ_r for the flanged termination is proportional to the square of frequency; this means that W_2 should increase with frequency, although W_1 will show a much weaker frequency dependence, especially at high amplitudes. Therefore, Δ_L may be expected to fall with frequency; at high amplitudes, this rate of decrease should be about 6 dB/octave. These arguments are borne out by the data, as one may see.

For $L_p^i = 150$ dB, Δ_L is equal to 30 dB at 500 Hz with the flanged termination but only 15 dB at the same frequency with the ρc termination. On the other hand, the rate of fall-off of Δ_L with frequency is greater in the case of the flanged termination. Equations (3) and (8) indicate that if θ_{NL} dominates ζ_1, then W_{abs} will be mainly dependent on L_p^i and not on θ_r. Therefore, the *actual* power dissipated should not depend markedly upon θ_r; W_2, however, is largely dependent upon θ_r and represents the acoustic power that "leaks away" from the orifice flow.

Figures 6 and 7 show data on the transmission loss Δ_T for orifices of diameter 3.3 and 6.35 mm, repectively, both with ρc terminations. Agreement between measurement and theory is good, and one sees that the larger orifice has a generally lower Δ_T, as would be expected. There is a tendency for Δ_T to rise with frequency for both orifices, because the $k_0\delta$ term in

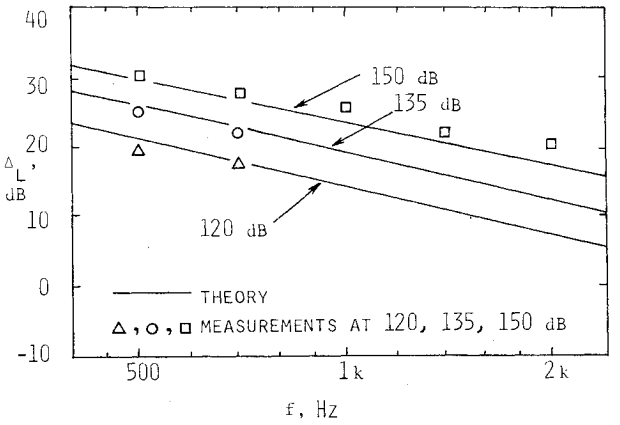

Fig. 5 Net power loss vs frequency for 3.3 mm orifice with flanged termination.

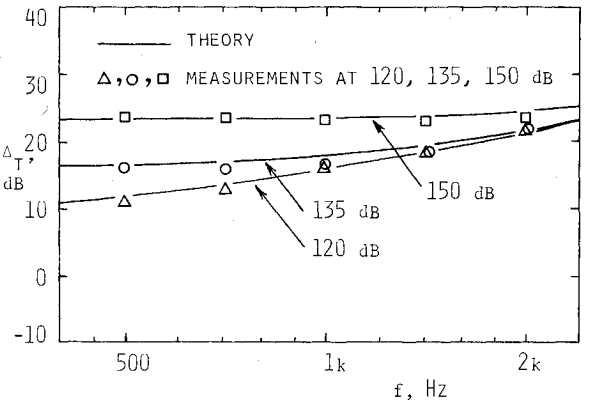

Fig. 6 Transmission loss vs frequency for 3.3 mm orifice with ρc termination.

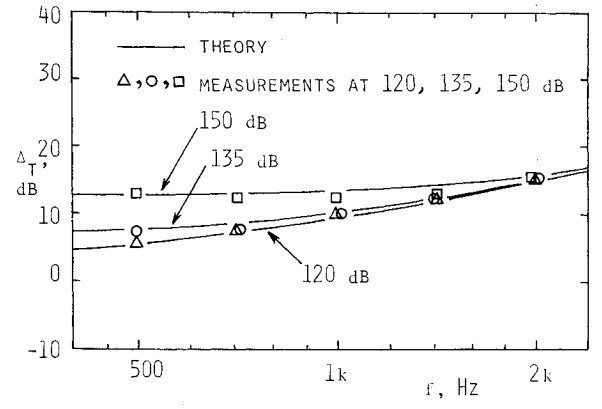

Fig. 7 Transmission loss vs frequency for 6.35 mm orifice with ρc termination.

ζ_1 increases, although this effect is suppressed at higher amplitudes. In both cases, Δ_T shows a dependence on L_p^i, which is strongest in the case of the smaller orifice and at low frequencies.

Altogether six orifices were tested, with diameters of 1.6-25.4 mm. Nonlinear transmission effects were observed in all of these, although the effects were most marked with the smaller orifices and at the lower frequencies.

Vortex Formation

Figure 8 shows a photograph of a train of ring vortices formed on the transmission side of a 12.7 mm diam orifice at 100 Hz, with $\hat{v} = 4$ m/s. The vortices are quite clearly defined,

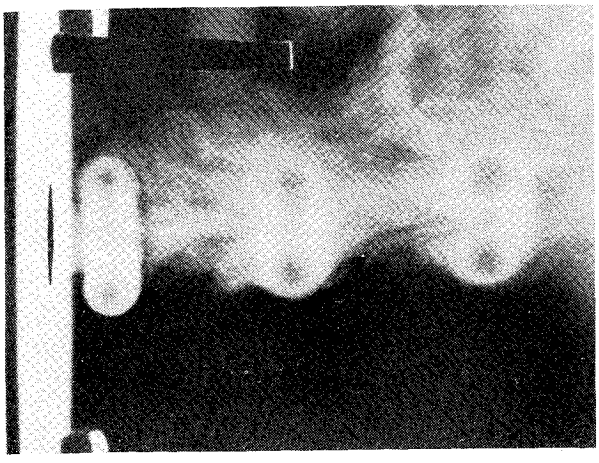

Fig. 8 Train of vortices on transmission side of 12.7 mm orifice ($f = 100$ Hz, $\hat{v} = 4$ m/s).

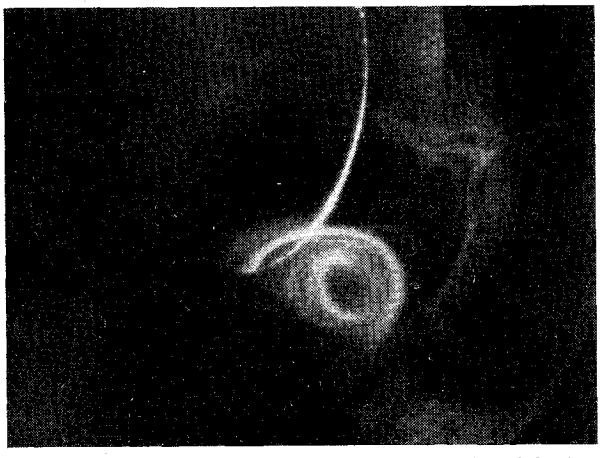

Fig. 9 Early stages of vortex roll-up on source side of 25.4 mm orifice ($f = 40$ Hz).

especially close to the orifice, while some diffusion of the vortex fluid into the surrounding air is evident farther away from the orifice. A *vena contracta* can be detected, approximately one orifice radius from the plate, and the wall effect is clearly evident, since the vortex closest to the plate has a radius about 20% greater than the other two. The object attached to the plate above the orifice is a scale indicator 30 mm long.

Figure 9 shows the early stages in a vortex roll-up at the 25.4 mm orifice for a frequency of 40 Hz. This photograph was taken from the source side of the orifice, through the wall of the Plexiglass tube. A single filament of smoke was injected below the orifice lip on the transmission side of the plate, and the spiral shape represents a streakline in a plane containing the axis of the vortex. The crescent-shaped line is part of the orifice lip. It would appear that the fluid leaves the orifice lip tangentially as the boundary layer separates, and then the flow changes direction to pass through the orifice. From this and other observations one may surmise that the Kutta condition is satisfied at the orifice lip during the roll-up process. No doubt the flow pattern is much more complex during an inflow/outflow changeover, although not enough data are available for any descriptive details to be given. Photographs take by Didden[18] suggest that the induced flow from each vortex might generate a secondary vortex of opposite circulation just before the flow changeover. This new vortex could be the nascent vortex of the succeeding, opposite, flow half-cycle.

Figures 10 and 11 show some comparisons between the measured vortex translational velocity as a function of peak

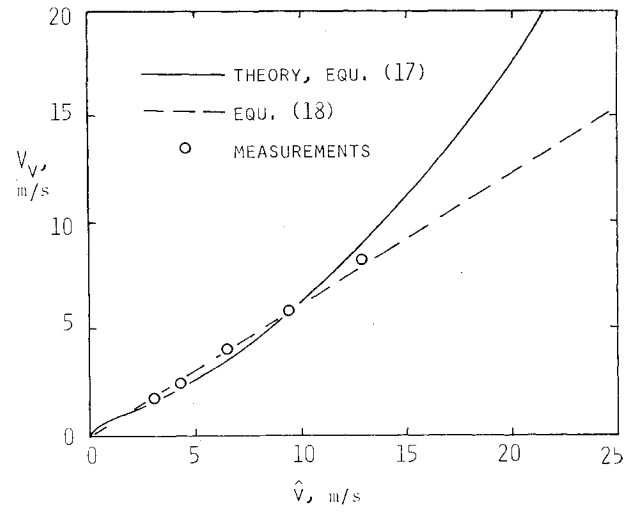

Fig. 10 Vortex translational velocity vs peak orifice velocity for 3.3 mm orifice ($f = 400$ Hz).

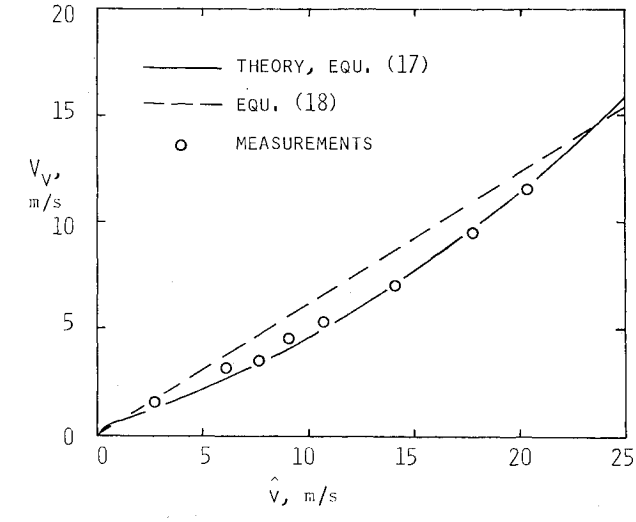

Fig. 11 Vortex translational velocity vs peak orifice velocity for 12.7 mm orifice ($f = 200$ Hz).

orifice velocity and theoretical predictions based on Eqs. (13) and (17). The orifice diameters are 3.3 and 12.7 mm and the frequencies 400 and 200 Hz, respectively. The theoretical curves are in good agreement with the measurements, especially considering the sensitivity of V_v to α and $\hat{v}$ [see Eq. (17)]. Not all of the comparisons showed such close agreement, but the theory generally gave reasonably good predictions in view of the possible uncertainties in Eq. (13) and the experimental errors incurred in the measurement of $\hat{v}$. One can infer that Eq. (17), and the physical arguments associated with it, bear at least some semblance to reality.

A number of sets of measurements of V_v and $\hat{v}$ was taken, and it was noticed that the relationship between the experimental values of V_v and $\hat{v}$ was approximately linear, in general, over the range of measurement. Therefore, a straight-line fit was made to all of the data, resulting in the empirical relationship

$$V_v = 0.62\hat{v} \tag{18}$$

This relationship gave a tolerably good fit to most of the experimental data and implies that the vortices travel at about 0.62 of the peak orifice velocity. One notes that, in the case of round turbulent jets, the eddy convection velocity, divided by the jet velocity, is typically of this order; in the data of Davies,

Fisher, and Barratt,[19] for example, this figure is about 0.65. Whether this implies that there is any similarity between the mechanism of eddy formation in a turbulent jet and vortex roll-up at an orifice is, of course, an open question.

It might, perhaps, be tempting to take Eq. (18) and work back through the theory in Sec. II to obtain an expression for the nonlinear resistance, but this does not, in fact, give sensible results because of the absence of a quadratic term in $\hat{v}$ from Eq. (18).

V. Discussion

The theory for high-amplitude acoustic transmission at orifices is in reasonably good agreement with the measured data taken using tone bursts. This is to be expected on the basis of the favorable comparisons made by Cummings and Eversman[10] between theoretical predictions and measurements made with transient signals having a broad frequency spectrum. In this latter case, some doubt was expressed concerning the validity of using Fourier transformed data on a nonlinear system, but even so, theory and measurement were in quite good agreement. In the present case, since most of the energy in the tone burst is in a narrow frequency band, this objection does not arise. This is, in fact, one of the reasons for using tone burst excitation in the present study; an additional reason is that considerations of periodically shed vortices can more readily be reconciled with those of energy dissipation in a periodic orifice flow.

It has been shown that the loss of acoustic power at the orifice is consistent with the transfer of this power into the kinetic energy of two trains of ring vortices shed alternately from both sides of the orifice. Predictions of the vortex translational velocity made on this basis are in generally reasonable agreement with the measurements, albeit isolated vortex models were used in the process.

The nonlinear interaction of sound waves with orifices is obviously a more complicated process than the simplified theoretical models described here would suggest. For example, the role of viscosity has been largely suppressed, although viscous effects must, of course, play a part in the phenomenon. Also, the distribution of vorticity implicit in the models is unlikely to be an exact representation of the actual process; this view is supported by the extensive measurements of Didden[18] on single vortices. Despite this, it is felt that the essential features of the nonlinear behavior of orifices have been preserved and that useful theoretical results have been obtained.

One practical aspect of the present work concerns acoustic attenuators that incorporate perforated structures. In general, both mean flow and complex acoustic waveforms would exist, and it would seem logical to extend the present study in these directions. The role of mean tangential flow and through flow in determining the impedance of both singly and multiply perforated plates can usefully be examined. The effects of sound fields incorporating pure tones, combinations of tones, random noise, and broadband impulsive signals should be investigated experimentally and appropriate theoretical models devised.

Acknowledgment

This research was supported by a University of Missouri Weldon Springs Research Award.

References

[1] Bechert, D. W., Michel, U., and Pfizenmaier, E., "Experiments on the Transmission of Sound through Jets," AIAA Paper 77-1278, Oct. 1977.

[2] Ahuja, K. K., Salikuddin, M., and Plumblee, H. E., "Characteristics of Internal- and Jet-Noise Radiation from a Multi-Lobe, Multi-Tube Suppressor Tested Statically and under Flight Simulation," AIAA Paper 80-1027, June 1980.

[3] Bechert, D. W., "Sound Absorption Caused by Vorticity Shedding Demonstrated with a Jet Flow," AIAA Paper 79-0575, March 1979.

[4] Howe, M. S., "Attenuation of Sound in a Low Mach Number Nozzle Flow," *Journal of Fluid Mechanics,* Vol. 91, March 1979, pp. 209-229.

[5] Howe, M. S., "The Dissipation of Sound at Sharp Edges," AIAA Paper 80-0972, June 1980.

[6] Rienstra, S. W., "On the Acoustical Implications of Vortex Shedding in an Exhaust Pipe," ASME Paper 80-WA/NC-16, Nov. 1980.

[7] Salikuddin, M. and Plumblee, H. E., "Low Frequency Sound Absorption of Orifice Plates, Perforated Plates, and Nozzles," AIAA Paper 80-0991, June 1980.

[8] Cummings, A. and Eversman, W., "Acoustic Dissipation on Radiation through Duct Terminations—Theory," AIAA Paper 81-1979, Oct. 1981.

[9] Cummings, A., "High-Amplitude Acoustic Power Losses in Perforated Materials," ASME Paper 81-WA/NCA-10, Nov. 1981.

[10] Cummings, A. and Eversman, W., "High Amplitude Acoustic Transmission through Duct Terminations: Theory," *Journal of Sound and Vibration,* Vol. 91, Dec. 1983, pp. 503-518.

[11] Hersh, A. S. and Rogers, T., "Fluid Mechanical Model of the Acoustic Impedance of Small Orifices," NASA CR-2682, 1976.

[12] Ingard, U. and Labate, S., "Acoustic Circulation Effects and the Nonlinear Impedance of Orifices," *Journal of the Acoustical Society of America,* Vol. 22, March 1950, pp. 211-218.

[13] Disselhorst, J. H. M. and Van Wijngaarden, L., "Flow in the Exit of Open Pipes during Acoustic Resonance," *Journal of Fluid Mechanics,* Vol. 99, July 1980, pp. 293-319.

[14] Saffman, P. G., "On the Formation of Vortex Rings," *Studies in Applied Mathematics,* Vol. 54, Sept. 1975, pp. 261-268.

[15] Sommerfeld, A., *Mechanics of Deformable Bodies,* Academic Press, New York, 1964.

[16] Maxworthy, T., "Some Experimental Studies of Vortex Rings," *Journal of Fluid Mechanics,* Vol. 81, July 1977, pp. 465-495.

[17] Leiss, C. and Didden, N., "Experimentelle untersuchung von ringwirbeln," 50 Jahre M.P.I. Strömungsforschung, Göttingen, FRG, 1975.

[18] Didden, N., "On the Formation of Vortex Rings: Rolling-up and Production of Circulation," *Journal of Applied Mathematics and Physics (ZAMP),* Vol. 30, 1979, pp. 101-116.

[19] Davies, P. O. A. L., Fisher, M. J., and Barratt, M. J., "The Characteristics of the Turbulence Produced in the Mixing Region of a Round Jet," *Journal of Fluid Mechanics,* Vol. 15, 1963, pp. 337-367.